Human Genomics

RESEARCH

Open Access

Bioinformatics analysis of circular RNAs associated with atrial fibrillation and their evaluation as predictive biomarkers

Manman Wang[1,2†], Yuanyuan Chen[1†], Weiwei Yang[3†], Xiangting Li[1], Genli Liu[1], Xin Wang[1], Shuai Liu[1], Ge Gao[1], Fanhua Meng[1], Feifei Kong[4], Dandan Sun[1], Wei Qin[5], Bo Dong[6*] and Jinguo Zhang[1*]

Abstract

Background Circular noncoding RNAs (circRNAs) are implicated in many human diseases, but their role in atrial fibrillation (AF) is poorly understood. In this study, we performed bioinformatics analysis of circRNA sequencing data to identify AF-related circRNAs.

Methods Left atrial appendage (LAA) samples were obtained from patients with valvular heart disease and were categorised into the sinus rhythm (SR; n = 4) and AF (n = 4) groups. CircRNA sequencing analysis was performed to identify differentially expressed (DE) circRNAs in AF patients. Functional enrichment analysis of DE circRNAs was performed to identify enriched Gene Ontology (GO) terms and Kyoto Encyclopedia of Genes and Genomes (KEGG) pathways.

Results We identified 3338 DE circRNAs, including 2147 upregulated and 1191 downregulated circRNAs, in AF patients. A ceRNA network of 16 DE circRNAs, 11 DE miRNAs, and 15 DE mRNAs was constructed. Functional enrichment analyses revealed that the AF-related DE circRNAs were enriched in response to vitamin D, the potassium channel complex, delayed rectifier potassium channel activity, osteoclast differentiation, primary immunodeficiency, endocrine and other factor-regulated calcium reabsorption and other processes. ROC curve analysis identified circRNA_00324, circRNA_17225, circRNA_16305, circRNA_10233, circRNA_05499, circRNA_03183, circRNA_14211, and circRNA_18422 as potential predictive biomarkers for distinguishing AF patients from SR patients, with AUC values of 0.9138, 0.7370, 0.8526, 0.6803, 0.8163, 0.8662, 0.7664, and 0.9320, respectively.

Conclusions In this study, we constructed an AF-related ceRNA network and identified eight circRNAs as potential predictive biomarkers of AF.

Keywords Atrial fibrillation, Circular RNA, Bioinformatic analysis, Competing endogenous RNA, Biomarker

†Manman Wang, Yuanyuan Chen and Weiwei Yang contributed equally to this work and share first authorship.

*Correspondence:
Bo Dong
bodong@sdu.edu.cn
Jinguo Zhang
zhangjinguo@mail.jnmc.edu.cn
Full list of author information is available at the end of the article

© The Author(s) 2025. **Open Access** This article is licensed under a Creative Commons Attribution-NonCommercial-NoDerivatives 4.0 International License, which permits any non-commercial use, sharing, distribution and reproduction in any medium or format, as long as you give appropriate credit to the original author(s) and the source, provide a link to the Creative Commons licence, and indicate if you modified the licensed material. You do not have permission under this licence to share adapted material derived from this article or parts of it. The images or other third party material in this article are included in the article's Creative Commons licence, unless indicated otherwise in a credit line to the material. If material is not included in the article's Creative Commons licence and your intended use is not permitted by statutory regulation or exceeds the permitted use, you will need to obtain permission directly from the copyright holder. To view a copy of this licence, visit http://creativecommons.org/licenses/by-nc-nd/4.0/.

Introduction

Atrial fibrillation (AF) is the most common type of persistent arrhythmia in clinical practice and is known as a "cardiovascular epidemic of the twenty-first century." AF is associated with high mortality rates and incidences of stroke, heart failure, and cognitive dysfunction [1]. The incidence of AF is increasing globally. The worldwide estimates from the Global Burden of Disease (GBD) study revealed that 59.7 million people were diagnosed with AF in 2019 [2]. The primary treatment strategy for AF includes drug therapy for controlling heart rhythm and preventing thrombosis. However, this therapeutic strategy is associated with issues related to the maintenance of the sinus rhythm (SR) and several adverse effects. Currently, improving atrial remodelling is the central focus of drug research regarding AF. Therefore, unravelling the mechanisms underlying AF is necessary to identify novel intervention targets for AF and discover precise, targeted treatments for AF.

Circular RNAs (circRNAs) are a category of noncoding RNAs that are 200 to 100,000 nucleotides in length. They are generated by spliceosome-mediated pre-mRNA back-splicing of exons or introns. They lack a 5'-terminal m7G cap and a 3'-terminal polyadenosine tail because the downstream splice donor site (5' splice site) is covalently linked to an upstream acceptor splice site (3' splice site), which results in the formation of a closed circular loop. Therefore, circRNAs have longer half-lives than their linear RNA counterparts do and are less susceptible to degradation by RNA exonucleases [3]. Because of their unique features, circRNAs are more stable than linear RNAs are and play crucial functional roles in specific tissues and cells [4].

CircRNAs perform several biological functions. CircRNAs are best characterised as competitive endogenous RNAs (ceRNAs) because they competitively bind to specific microRNAs (miRNAs) and regulate gene expression [5]. In the ceRNA network, several noncoding RNAs, including circRNAs, competitively bind to specific miRNAs and modulate target gene expression [6]. CircRNAs play important roles as ceRNAs in the pathological and physiological processes of various human diseases, including cancer [7], endocrine and metabolic disorders [8], and cerebrovascular diseases [9]. Although the gene regulatory functions of circRNAs via complex interactions between circRNAs and other RNA molecules have been well established, the mechanisms underlying the roles of circRNAs in human cardiovascular diseases are poorly understood.

Therefore, in this study, we analysed circRNA sequencing data from AF and SR patients to identify AF-associated circRNAs. We subsequently constructed an AF-associated ceRNA network comprising AF-related circRNAs, miRNAs, and mRNAs. We assessed the diagnostic value of eight AF-related circRNAs via receiver operating characteristic (ROC) curve analysis.

Methods

Patient selection and sample collection

Left atrial appendage (LAA) tissues were collected from patients who underwent surgery for valvular heart disease at the Department of Cardiac Surgery of the Affiliated Hospital of Jining Medical University (Shandong, China) between January 2021 and April 2021. Patients were categorised into persistent AF (n = 4) and SR (n = 4) groups on the basis of their electrocardiogram results and medical history. Five millilitres of fasted peripheral whole blood samples were collected from patients with AF (n = 21) and SR (n = 21) and stored in EDTA tubes. The inclusion criteria for the patients were as follows: (1) satisfied the diagnostic criteria for persistent AF according to the 2020 ESC guidelines for the diagnosis and management of AF [1]; and (2) aged 18–80 years. The exclusion criteria were as follows: (1) a history of catheter ablation; (2) a history of coronary heart disease; (3) a left ventricular ejection fraction (LVEF) < 40%; (4) infectious diseases; (5) malignant tumours; (6) hyperthyroidism; (7) a history of stroke; and (8) severe liver or kidney dysfunction. This study was conducted according to the guidelines of the Declaration of Helsinki, and this research protocol was approved by the Ethics Committee of the Affiliated Hospital of Jining Medical University (Approval number: 2021B116). Written informed consent was obtained from each patient.

CircRNA sequencing analyses

Eight LAA samples (4 from each group) were sent to Shanghai OE Biomedical Science and Technology Company (Shanghai, China) for transcriptome sequencing via high-throughput sequencing technology. Total RNA was extracted from samples using TruSeq Stranded Total RNA with Ribo-Zero Gold capsules (Illumina, San Diego, CA, USA). Approximately 2–5 μg total RNA from each specimens was used for library construction. RNA integrity was analysed using an Agilent 2100 Bioanalyzer (Agilent Technologies, Santa Clara, CA, USA). Samples with an RNA integrity number (RIN) ≥ 7.0 were chosen for sequencing on an Illumina HiSeq™ 2500 sequencing platform (Illumina), and 150 bp/125 bp paired-end reads were generated.

CircRNA prediction and differential expression analysis

We referenced *Homo sapiens* circRNA sequences from the circBase (http://www.circbase.org/), CIRCpedia v2 (http://www.picb.ac.cn/rnomics/circpedia), and circAtlas (https://ngdc.cncb.ac.cn/circatlas) databases and

aligned them against gene annotation data and reference sequences using CIRI2 software [10] to identify candidate circRNA transcripts. The relevant code has been uploaded to a GitHub repository (https://github.com/fjxc1893/wRNAseq). We used Bedtools software [11] to classify the positional relationships between circRNA transcripts and known protein-coding transcripts. The raw circRNA data were subsequently filtered based on counts, and circRNAs with an average count > 2 were retained for further analysis to obtain high-quality data. The expression levels of the transcripts were determined via the use of junction reads per million mapped reads (RPM) to quantify the circRNAs, and the RPM statistical results of the circRNAs in each sample were displayed via a box–whisker plot. DEGseq software [12] was used to standardise the RPM of each sample circRNA, calculate the difference multiple, and use a negative binomial (NB) distribution test to evaluate the difference significance of the RPM. The Benjamini–Hochberg (BH) method was used to calculate the false discovery rate (FDR), and the p value was adjusted to obtain more reliable differentially expressed genes (DEGs). Finally, different circRNAs were screened according to the difference multiple and difference significance test results. The differentially expressed (DE) circRNAs were screened using $q < 0.05$ and |log2-fold change (FC)| > 1 as threshold parameters.

CeRNA network construction

Owing to the presence of multiple miRNA binding sites in circRNAs, miRNA target gene prediction can be used to identify circRNAs that bind to miRNAs, and the functions of these circRNAs can be elucidated on the basis of miRNA target gene functional annotation. Therefore, we constructed a circRNA-related ceRNA network. We first predicted the coexpression and regulatory relationships between the DE miRNAs and DE circRNAs. Pearson's rank correlation coefficient was used to identify the DE circRNA–miRNA pairs with negative correlations. The miRanda program [13] was used to predict interactions between the miRNAs and circRNAs. We subsequently identified DE miRNA–mRNA pairs and calculated the ceRNA scores using the MuTaME method [14]. According to the ceRNA hypothesis, circRNAs are positively correlated with mRNA expression levels [5]. Therefore, we performed Pearson's correlation analysis to identify circRNA–mRNA pairs with positive coexpression relationships. We subsequently performed enrichment analysis of the ceRNA score results and the regulatory relationships between DE circRNAs and DE miRNAs. Finally, we obtained a highly reliable ceRNA network and constructed an AF-related ceRNA network using Cytoscape software 3.10.1 (http://cytoscape.org/). A ceRNA network analysis flowchart is shown in Fig. 1.

Functional enrichment analyses of DEGs

Functional enrichment analyses of DEGs in the ceRNA networks were performed using Gene Ontology enrichment analysis (GO; http://geneontology.org/) and the Kyoto Encyclopedia of Genes and Genomes (KEGG; https://www.kegg.jp/) databases. DEGs and ceRNA networks with p values < 0.05 were considered significantly enriched.

Validation of circRNAs and ROC curve analysis

The total RNA of each LAA sample was extracted using TRIzol® reagent (Invitrogen, USA), and the total RNA of each blood sample was isolated via an RNAsimple Total RNA Kit (Catalogue No: DP419, TIANGEN, Beijing, China) according to the manufacturer's instructions. The RNA quantity and quality were determined using a NanoDrop 2000 spectrophotometer (Thermo Fisher Scientific, Waltham, MA, USA). A 260/280 nm absorbance ratio between 1.8 and 2.1 or a 260/230 nm absorbance ratio > 1.8 was considered acceptable. The RNA samples were subsequently reverse transcribed into cDNA using a FastQuant RT Kit (TIANGEN). Quantitative polymerase chain reaction (qPCR) analysis was performed to estimate the relative expression levels of the circRNAs using a SYBR Green Premix Pro Taq HS qPCR Kit (Accurate Biology, Hunan, China). PCR amplification was performed under the following cycling conditions: denaturation at 95 °C for 30 s, 45 cycles of 95 °C for 5 s and 60 °C for 30 s. qRT–PCR was performed on an ABI QuantStudio™ real-time PCR machine (Applied Biosystems, Foster City, CA, USA). Glyceraldehyde 3-phosphate dehydrogenase (*GAPDH*) was used as a reference gene for the expression levels of the circRNAs and mRNAs. The sequences of the RNA primers are shown in Table 1. Relative expression levels of genes were estimated using the $2^{-\Delta\Delta Ct}$ method. The analysis was repeated at least three times.

Furthermore, the predictive value of the candidate circRNAs was analysed using receiver operating characteristic (ROC) curves, and the area under the curve (AUC) values and 95% confidence intervals (CIs) were calculated.

Statistical analysis

The data were presented as the means ± standard errors of the means (SEMs). The statistical significance was measured using unpaired t tests (comparisons between two groups) and one-way ANOVA with Tukey's multiple comparisons test or repeated-measures ANOVA with the Bonferroni post hoc correction (multiple comparisons). Categorical variables were presented as numbers and percentages and were analysed using the chi-square

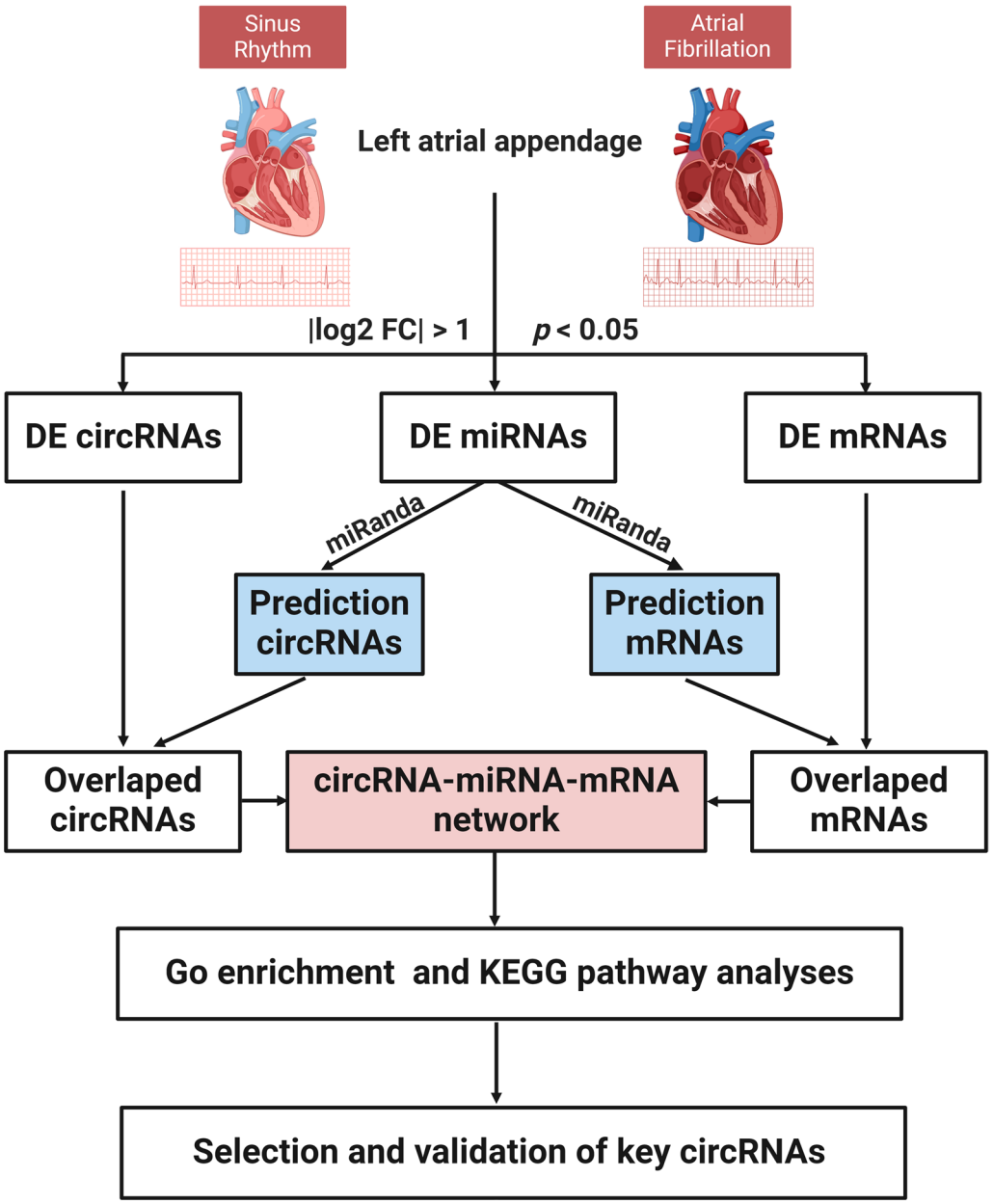

Fig. 1 Schematic representation of the bioinformatics analysis strategy used in this study

test or Fisher's exact test. $p < 0.05$ was considered statistically significant. SPSS version 29.0 (SPSS Inc., Chicago, IL, USA) and GraphPad Prism 9.0 (GraphPad, San Diego, CA, USA) were used for statistical analyses and generation of publication-quality graphs.

Results

Characterization of human circRNAs

In the present study, whole-transcriptome sequencing yielded 109.46 gigabases (G) of high-quality, clean data across all the samples. The RINs for individual samples ranged from 8.4 to 8.9, indicating well-preserved RNA quality. Each sample generated between 12.56 G and 14.41 G of valid sequencing data, with base call accuracies exceeding the Q30 thresholds of 95.32–95.57% of the nucleotides. The average guanine and cytosine (GC) content across datasets was 48.53% (Table S1). We identified 19,319 circRNAs, and the corresponding sequences of these circRNAs are shown in the Supplementary Material. Principal component analysis (PCA) revealed

Table 1 Primers used in the study

RNA	CircBase_id	Sequence (5′ → 3′)	Tm (°C)
circRNA_00324	hsa_circ_0004709	F: AGGAGTCAGAACCAGTACCTGT	60.0
		R: CAATGCGAGAGAACATGTAACCA	
circRNA_17225	N/A	F: CACTGAAGGTACTCTGCACCC	60.0
		R: TGTCGTCAAAGTCTGCCTTGT	
circRNA_16305	hsa_circ_0134845	F: GCAACATACCAGACCACTCTGC	60.0
		R: TGATGATTTGGGGAGAAGGGGC	
circRNA_10233	N/A	F: AAGTGCCTGAAGTGCTGCC	60.0
		R: GACCCACCGATTTTGCATTCATACC	
circRNA_05499	hsa_circ_0101642	F: TATGTACCGAAGGACTCTACCG	60.0
		R: CTTTGTATTTCCCTCATTTCTGTGC	
circRNA_03183	hsa_circ_0021506	F: CGGCAGGAGCTCTTCCTCA	60.0
		R: TGCTGCTCAGGCTCTGCTC	
circRNA_14211	hsa_circ_0071616	F: CGAGCTCTAATGACAAGCTCATGTAC	60.0
		R: AGAAGGAGCAGAAGCAGGAGC	
circRNA_18422	hsa_circ_0008038	F: GCACACTGGGAAGCTAGTATGT	60.0
		R: ATCATCTGTGCAGCAAGGTCA	
GAPDH	N/A	F: GCACCGTCAAGGCTGAGAAC	60.0
		R: TGGTGAAGACGCCAGTGGA	

that the SR and AF groups formed independent clusters (Fig. 2A). CircRNAs were quantified based on junction RPMs. The expression levels of all the circRNAs across the 8 samples from the two groups are shown in the box-whisker plot based on $\log_{10}$ (RPM + 1), and the results reveal no abnormal expression patterns across the 8 sample groups (Fig. 2B). On the basis of the positional relationships between the circRNAs and known protein-coding transcripts, the circRNAs were classified into the following types: antisense circRNAs, 304 (1.57%); exonic circRNAs, 680 (3.52%); intergenic circRNAs, 867 (4.49%); intronic circRNAs, 248 (1.28%); and sense-overlapping circRNAs, 17,220 (89.14%) (Fig. 2C). Our data reveal that these circRNAs are widely distributed across all chromosomes (Fig. 2D). Most of the circRNAs (15,107; 78.20%) were 200–2000 bp in length (Fig. 2E). Furthermore, 2,344 (12.13%) of the circRNAs consisted of a single exon, whereas the remaining circRNAs consisted of multiple exons (Fig. 2F). These results demonstrated the differential and characteristics of circRNAs between the SR and AF groups.

Expression profiles of circRNAs

Our data revealed that 3338 out of the 19,319 circRNAs were differentially expressed in the LAA tissues of patients with AF compared with those of SR patients based on threshold parameters $|\log2\ FC| > 1$ and $q < 0.05$ (Table S2). Furthermore, among these 3338 DE circRNAs, 2147 showed upregulated expression and 1191 showed downregulated expression (Fig. 3A). The volcano maps and heatmaps of the DE circRNAs are shown in Fig. 3B-C.

Construction of the ceRNA network

We set the correlation analysis threshold to a correlation coefficient ≥ 0.80 and $p \leq 0.05$. A total of 2,949 circRNA–miRNA pairs were screened. Furthermore, based on the interactions between circRNAs and miRNAs, negative regulatory relationship pairs were screened, and ultimately, 87 circRNA–miRNA pairs were obtained (Table S3). Similarly, we performed coexpression analysis of the DE miRNA–DE mRNA and DE circRNA–DE mRNA pairs and identified 109 miRNA–mRNA pairs with negative regulatory relationships and 89,997 circRNA–mRNA pairs with positive regulatory relationships (Table S4–6). The intersection between the ceRNA scores and the DE circRNA-DE mRNA coexpression results revealed a total of 62 DE circRNA-DE miRNA-DE mRNA relationship pairs after filtering, and the results are presented in a Venn diagram (Fig. 4A; Table S7). We then used Cytoscape software to construct a ceRNA network with 16 circRNAs, 11 miRNAs, and 15 mRNAs (Fig. 4B; Table S8).

Functional and pathway enrichment analyses

GO and KEGG enrichment analyses were used to determine the biological functions of the DEGs in the ceRNA network (Table S9 and S10). GO analysis revealed that the DEGs were enriched in 35 GO-biological process terms, 19 GO-cellular component

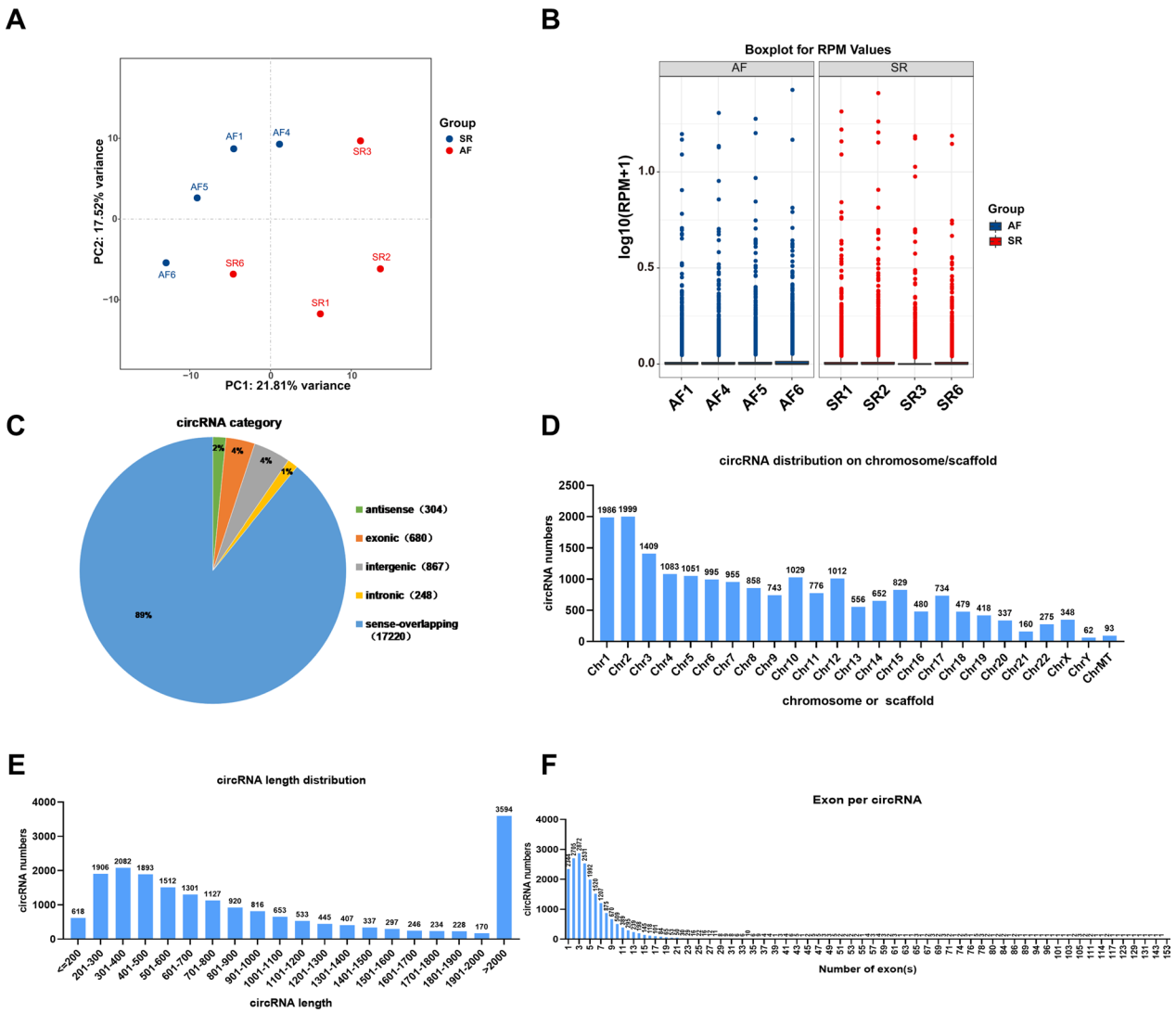

Fig. 2 Transcriptome sequencing analysis of DE circRNAs in the SR and AF groups. **A** Principal component analysis (PCA) of samples from the SR and AF groups. **B** Boxplot of RPM values for the circRNAs in the SR and AF samples. **C** Classification of circRNAs and proportion of different circRNA types. **D** Chromosomal distribution of the circRNAs. **E** Length of circRNAs in the SR and AF groups. **F** Statistical chart shows the number of exons in the circRNAs. AF, atrial fibrillation; DE, differentially expressed; RPM, reads per million mapped reads; SR, sinus rhythm

terms, and 17 GO-molecular function terms. The top 30 GO terms are visualised using bubble plots. GO enrichment analysis revealed that DEGs were enriched in response to vitamin D, potassium channel complex, delayed rectifier potassium channel activity, regulation of store-operated calcium entry, and response to oxidative stress and other processes (Fig. 5A; Table 2). Pathway analyses revealed that the DEGs were enriched in osteoclast differentiation, primary immunodeficiency, and endocrine and other factor-regulated calcium reabsorption and other processes (Fig. 5B; Table 2).

Validation of key circRNAs in the ceRNA network

On the basis of the ceRNA hypothesis, circRNAs competitively bind to miRNAs through miRNA response elements (MREs), thereby inhibiting downstream target gene silencing by isolating miRNAs from mRNAs [15]. Thus, in the coexpression network diagram of ceRNAs, both circRNAs and mRNAs serve as MREs, and their expression levels are positively correlated with one another and negatively correlated with miRNAs [5]. To validate the sequencing results, we selected eight circRNAs with high ceRNA scores and performed qRT–PCR

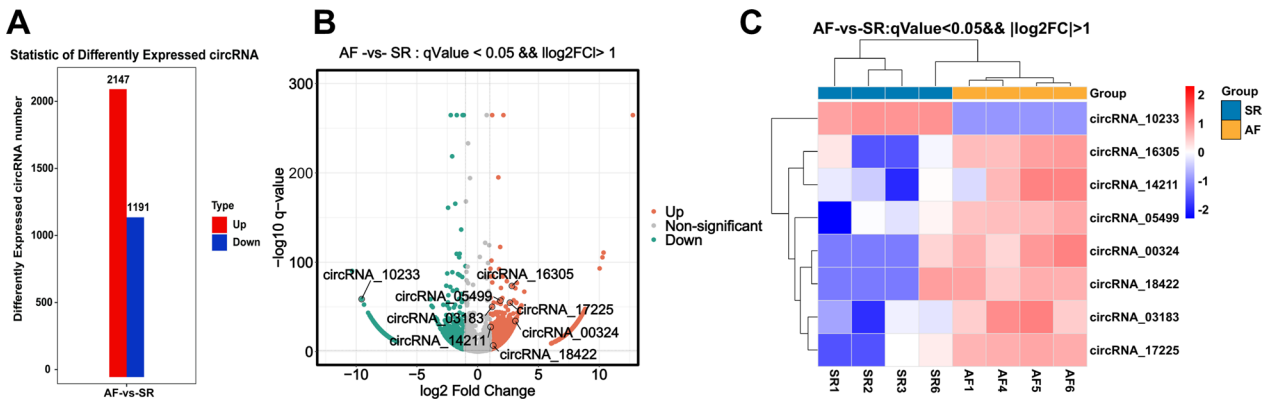

Fig. 3 Identification and characterization of the DE circRNAs. **A** Total number of DE circRNAs in the AF and SR groups. **B** Volcano plot showing 3,338 DE circRNAs with the threshold as |log2FoldChange|> 1 and *q*-value < 0.05. The green dot, red dot and gray dot represented the downregulated circRNAs (AF/SR), upregulated circRNAs and non-significant changed circRNAs, respectively. **C** Expression heatmap of the eight selected circRNAs in the two groups. AF, atrial fibrillation; SR, sinus rhythm; DE, differentially expressed

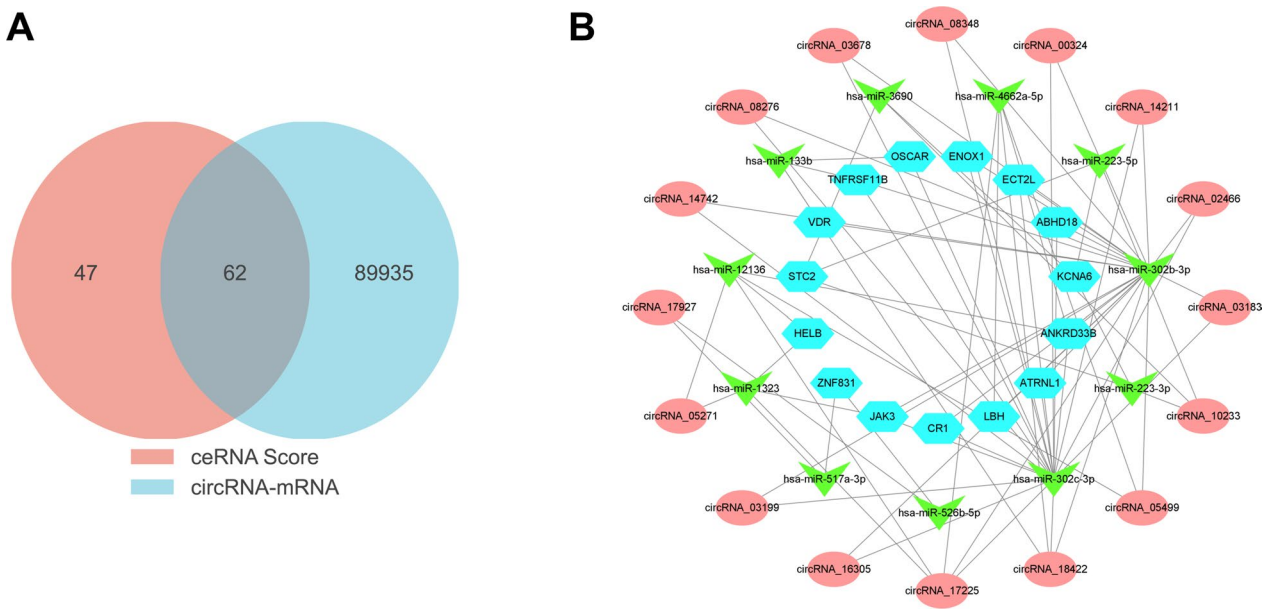

Fig. 4 The circRNA–miRNA–mRNA regulatory network. **A** Venn diagram shows the intersection analysis between the ceRNA score results and the co-expression analysis of DE circRNA–DE mRNA. **B** Construction of the circRNA–miRNA–mRNA regulatory network based on the ceRNA hypothesis. The light blue, green, and pink colors represent the mRNAs, miRNAs, and circRNAs, respectively. DE, differentially expressed

analysis of the LAA tissues. The qRT–PCR results revealed that the expression trends of the eight selected circRNAs were consistent with the sequencing results (Fig. 6A–B**;** Table 3). These findings suggest that the sequencing results were accurate. Blood samples can be used for analysing pathways associated with cardiovascular diseases [16]. Therefore, to further analyse the clinical diagnostic value of the selected circRNAs for AF patients, we estimated their expression levels in the whole peripheral blood of patients. The clinical characteristics of the patients are shown in Table 4. The eight selected circRNAs were differentially expressed in the peripheral blood of AF patients compared to those with SR ($p < 0.05$) (Fig. 6C). ROC curve analysis was subsequently performed to assess the predictive value of these circRNAs for distinguishing patients with AF from those with SR. The AUC values for circRNA_00324, circRNA_17225, circRNA_16305, circRNA_10233, circRNA_05499, circRNA_03183, circRNA_14211, and circRNA_18422 were 0.9138, 0.7370, 0.8526, 0.6803, 0.8163, 0.8662, 0.7664,

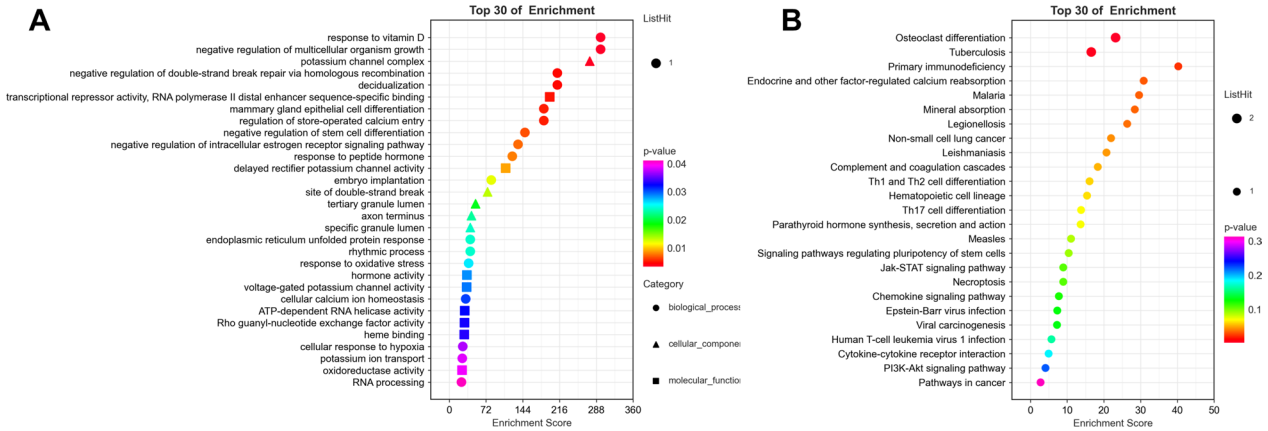

Fig. 5 GO annotation and KEGG pathway analyses of the target mRNAs. **A** Top 30 enriched terms according to GO analysis. **B** Top 30 enriched KEGG pathways

and 0.9320, respectively (Fig. 6D–G; Table 5). These results demonstrate optimal clinical diagnostic values for the eight candidate circRNAs. Therefore, these eight circRNAs are potential independent predictors of AF.

Discussion

The incidence of AF remains high despite significant advances and innovations in treatment strategies and drugs. In this study, we performed circRNA sequencing analysis of LAA tissues from 4 patients each with AF and SR and identified 3,338 DE circRNAs between the groups. Furthermore, we constructed a circRNA–miRNA–mRNA network of 16 circRNAs, 11 miRNAs, and 15 mRNAs and identified eight circRNAs with diagnostic value. These eight circRNAs may serve as potential biomarkers for the prediction, diagnosis, and treatment of AF.

CircRNAs regulate several biological processes and are ideal candidate diagnostic biomarkers in several human diseases because of their stability and conserved structures [17]. CircRNAs regulate tumorigenesis by interacting with transcription and growth factors [18]. They also act as ceRNAs by sponging specific miRNAs, thereby regulating the expression levels of downstream transcripts [19]. CircRNAs interact with several RNA-binding proteins and play a vital role in disease progression by regulating molecular signalling pathways [20]. CircRNAs regulate transcription and parent gene splicing by interacting with eukaryotic RNA Pol II [21]. Recent studies have also described the protein-encoding abilities of some circRNAs; the translation of circRNAs can be modulated through m6A modifications, and circRNAs can encode proteins or peptides in response to external stimulation [22]. Therefore, circRNAs play crucial roles in various biological processes by regulating gene expression and have potential as clinical biomarkers for various human diseases.

The roles of circRNAs in ceRNA regulatory networks have been investigated in mammals. CircRNA–miRNA–mRNA networks play critical roles in the pathophysiological processes of various heart diseases. For example, CircBPTF expression was upregulated in the left ventricular tissues of patients with end-stage ischaemic heart failure (IHF), and silencing CircBPTF expression inhibited the expression of *HDAC9* and *LRRC17* by targeting miR-196b-5p [23]. Circ_0001052 expression was significantly upregulated in a pathologic cardiac hypertrophy (CH) model established by aortic transverse contraction (TAC) and promoted cardiac hypertrophy by acting as a ceRNA for *Hipk3* through the sponging of miR-148a-3p and miR-124-3p [24]. In the present study, through the construction of an AF-specific ceRNA-mediated network and bioinformatic analyses, several important biological processes, such as the response to vitamin D, potassium channel complex, delayed rectifier potassium channel activity, regulation of store-operated calcium entry, response to oxidative stress, osteoclast differentiation, primary immunodeficiency, and endocrine and other factor-regulated calcium reabsorption, and other processes, were enriched. These findings support that the circRNA–miRNA–mRNA network established in the present study may be involved in regulating the occurrence and development of AF.

Atrial electrical remodelling is the electrophysiological substrate that results in the reentry excitation of AF, and this process is closely related to the dysfunction of ion channels [25]. Changes in some transmembrane ionic currents, such as the transient outwards potassium current (I_{to}), inwards sodium current (I_{NA}) and small conductance calcium-activated potassium channel current

Table 2 Top 30 enriched GO terms and KEGG pathways of DEGs in the ceRNA network

Term_ID	Term_description	Genes number	*p*-value	FDR
GO:0033280	Response to vitamin D	1	0.003371289	0.031399354
GO:0040015	Negative regulation of multicellular organism growth	1	0.003371289	0.031399354
GO:0034705	Potassium channel complex	1	0.00362976	0.068965444
GO:2000042	Negative regulation of double-strand break repair via homologous recombination	1	0.004716973	0.031399354
GO:0046697	Decidualization	1	0.004716973	0.031399354
GO:0001206	Transcriptional repressor activity, RNA polymerase II distal enhancer sequence-specific binding	1	0.005074496	0.076551439
GO:0060644	Mammary gland epithelial cell differentiation	1	0.005389209	0.031399354
GO:2001256	Regulation of store-operated calcium entry	1	0.005389209	0.031399354
GO:2000737	Negative regulation of stem cell differentiation	1	0.006732471	0.031399354
GO:0033147	Negative regulation of intracellular estrogen receptor signaling pathway	1	0.007403497	0.031399354
GO:0043434	Response to peptide hormone	1	0.008074119	0.031399354
GO:0005251	Delayed rectifier potassium channel activity	1	0.009006052	0.076551439
GO:0007566	Embryo implantation	1	0.012089406	0.042312922
GO:0035861	Site of double-strand break	1	0.013251933	0.091116667
GO:1904724	Tertiary granule lumen	1	0.019223761	0.091116667
GO:0043679	Axon terminus	1	0.022791418	0.091116667
GO:0035580	Specific granule lumen	1	0.02397807	0.091116667
GO:0048511	Rhythmic process	1	0.024048723	0.070079104
GO:0030968	Endoplasmic reticulum unfolded protein response	1	0.024048723	0.070079104
GO:0006979	Response to oxidative stress	1	0.026029382	0.070079104
GO:0005179	Hormone activity	1	0.02846472	0.081150976
GO:0005249	Voltage-gated potassium channel activity	1	0.029015834	0.081150976
GO:0006874	Cellular calcium ion homeostasis	1	0.030637029	0.075330472
GO:0004004	ATP-dependent RNA helicase activity	1	0.032316894	0.081150976
GO:0005089	Rho guanyl-nucleotide exchange factor activity	1	0.032866135	0.081150976
GO:0020037	Heme binding	1	0.033415108	0.081150976
GO:0071456	Cellular response to hypoxia	1	0.037185771	0.075330472
GO:0006813	Potassium ion transport	1	0.03849079	0.075330472
GO:0016491	Oxidoreductase activity	1	0.038890166	0.082641602
GO:0006396	RNA processing	1	0.041096112	0.075330472
KEGG pathway				
path:hsa04380	Osteoclast differentiation	2	0.00285353	0.069102014
path:hsa05152	Tuberculosis	2	0.005528161	0.069102014
path:hsa05340	Primary immunodeficiency	1	0.024602403	0.126881991
path:hsa04961	Endocrine and other factor-regulated calcium reabsorption	1	0.032022406	0.126881991
path:hsa05144	Malaria	1	0.033366633	0.126881991
path:hsa04978	Mineral absorption	1	0.034709365	0.126881991
path:hsa05134	Legionellosis	1	0.037390354	0.126881991
path:hsa05223	Non-small cell lung cancer	1	0.044732371	0.126881991
path:hsa05140	Leishmaniasis	1	0.047391061	0.126881991
path:hsa04610	Complement and coagulation cascades	1	0.053351471	0.126881991
path:hsa04658	Th1 and Th2 cell differentiation	1	0.06059586	0.126881991
path:hsa04640	Hematopoietic cell lineage	1	0.06321916	0.126881991
path:hsa04659	Th17 cell differentiation	1	0.070403028	0.126881991
path:hsa04928	Parathyroid hormone synthesis, secretion and action	1	0.071053915	0.126881991
path:hsa05162	Measles	1	0.087207982	0.144264907
path:hsa04550	Signaling pathways regulating pluripotency of stem cells	1	0.09232954	0.144264907
path:hsa04630	Jak-STAT signaling pathway	1	0.10692609	0.148508459

Table 2 (continued)

Term_ID	Term_description	Genes number	*p*-value	FDR
path:hsa04217	Necroptosis	1	0.10692609	0.148508459
path:hsa04062	Chemokine signaling pathway	1	0.122578288	0.1555122
path:hsa05169	Epstein-Barr virus infection	1	0.129395348	0.1555122
path:hsa05203	Viral carcinogenesis	1	0.130630248	0.1555122
path:hsa05166	Human T-cell leukemia virus 1 infection	1	0.162848038	0.185054589
path:hsa04060	Cytokine-cytokine receptor interaction	1	0.185939644	0.202108309
path:hsa04151	PI3K-Akt signaling pathway	1	0.221033041	0.230242751
path:hsa05200	Pathways in cancer	1	0.312492782	0.312492782

FDR, false discovery rate. DEGs, differentially expressed genes

(SK), are key determinants of electrical remodelling, and the I_{to} plays a major role in early repolarisation [26, 27]. Previous studies have confirmed that circRNAs can affect AF occurrence by regulating ion channel function. For example, in a mouse model of AF, mmu_circ_0005019 overexpression increased electrical remodelling by promoting the expression of Kcnd1 (encoding the I_{to}) and Scn5a and Kcnn3 (encoding the I_{NA} and SK3); mmu_circ_0005019 also served as a sponge for miR-499-5p by targeting *Kcnn3* [28]. In this study, we found that circRNAs can affect ion channel function in AF patients by regulating *KCNA6*, *STC2*, and *VDR* expression (Table S11). KCNA6 (encoding the Kv1.6 channel), which is expressed at low levels in working cardiomyocytes, is significantly expressed in human cardiac fibroblasts and is involved in regulating the proliferation of mouse cardiac c-kit (+) cells [29, 30]. The expression of STC2, a secreted glycoprotein hormone originally described in fish, in embryonic fibroblasts of mice increased susceptibility to endoplasmic reticulum (ER) and oxidative stress; STC2 functions as a negative regulator of Ca^{2+} influx through store-operated Ca^{2+} channels (SOCs) [31]. Vitamin D receptors (VDRs) are nuclear receptors and key mediators of the actions of 1,25(OH)2D3, including the regulation of calcium metabolism and intestinal calcium absorption [32]. *VDR* expression deficiency reduces calcium absorption by more than 70% [33]. Defective calcium absorption leads to calcium homeostasis disorders, which are also associated with increased susceptibility to AF.

CircRNAs are also associated with osteoclast differentiation, the response to oxidative stress, pathways involved in cancer, and primary immunodeficiency. Osteoclast differentiation plays a critical role in myocardial fibrosis, and osteoclasts are rich in mitochondria, which can generate reactive oxygen species (ROS) through components of the electron transport chain and NADPH oxidase [34, 35]. Mitochondrial dysfunction and elevated levels of ROS are closely related to the occurrence of AF [36]. In previous studies, it has been reported that tumours are associated with arrhythmias. Patients with malignant tumours have an increased risk of AF [37]. The incidence rate of AF is 1–2% in the general population but is increased to 5–16% in patients with tumours [38]. Elevated levels of cytokines and chemokines in the tumour microenvironment are associated with AF development and progression [39]. In addition, immune remodelling during AF involves aberrant recruitment, activation, and redistribution of immune cells in the atrium and abnormal secretion of immune factors [40]. Activated immune cells release several proinflammatory factors, including MIF, TNF-α, IL-1β, and IL-6, which induce atrial electrical and structural remodelling in AF patients [41].

Many circRNAs exhibiting cell type- or tissue-specific expression patterns have been identified in human body fluids [42]. Previous studies have shown that DE circRNAs in blood are potential prognostic biomarkers for cardiovascular diseases [43]. In this study, we verified the expression of several DE circRNAs in the peripheral blood of patients with AF. ROC curve analysis suggested that the eight DE circRNAs analysed were potential predictive biomarkers of AF. CircRNA_18422 interacts with hsa-miR-302b-3p and hsa-miR-302c-3p, which are members of the miR-302-3p family whose expression is downregulated in the right atrial appendages of AF patients and regulate atrial fibrosis by targeting *SDC-1* [44]. CircRNA_10233 interacts with miR-223-3p, whose expression is upregulated in AF patient tissues and regulates autophagy by targeting *FoxO3* [45]. *ENOX1* and other genes are also downstream targets of these selected circRNAs. *ENOX1* is a highly conserved NADH oxidase that catalyses the oxidation of NADH to NAD^+, dysregulation of *ENOX1* is associated with aberrant atrial structural and electrical remodelling, leading to the onset and persistence of AF [46, 47]. Therefore, the construction of a ceRNA network for AF-related circRNAs will help to

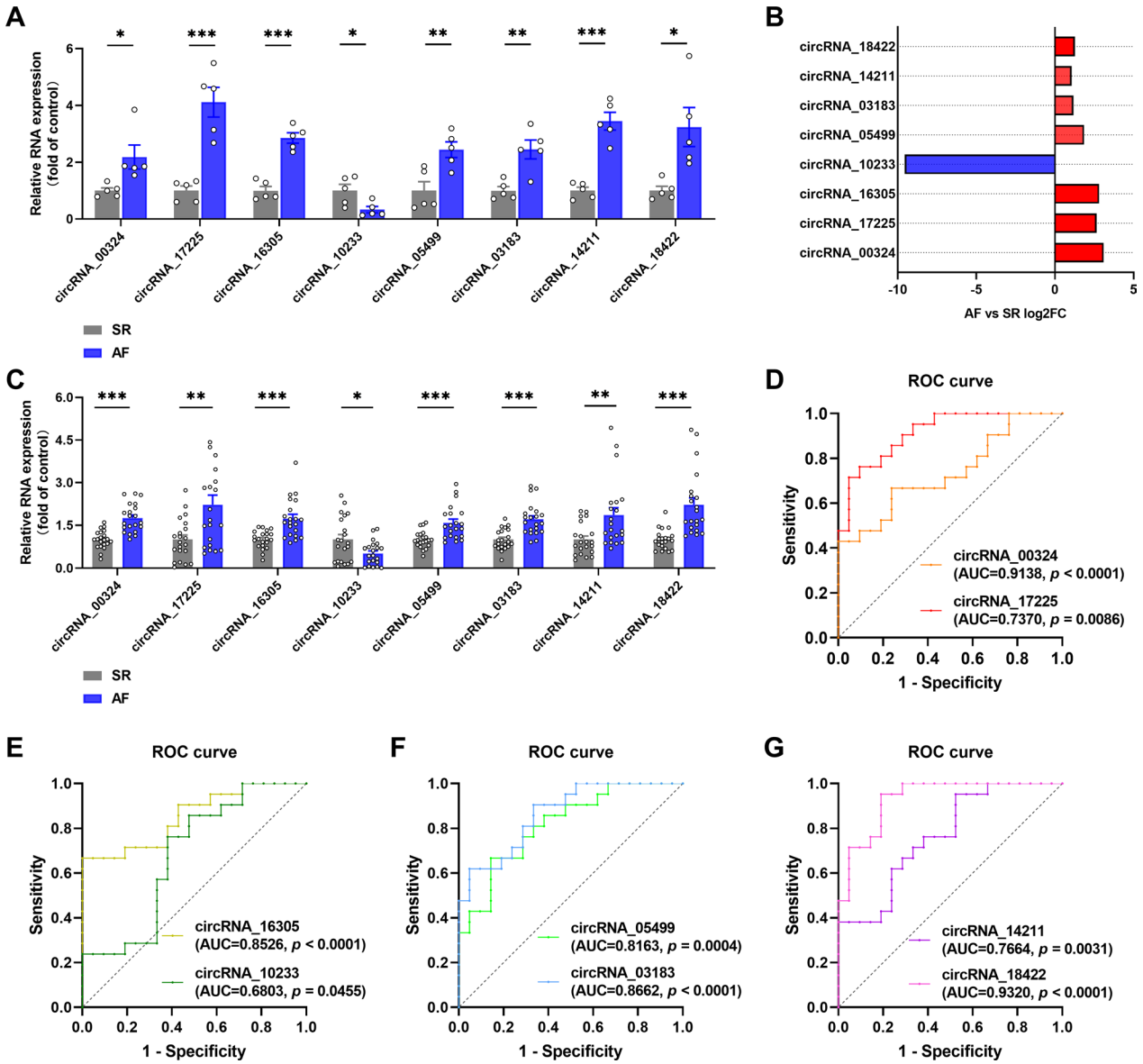

Fig. 6 Validation analysis of the eight DE circRNAs. **A** qRT-PCR analysis of the relative expression levels of the eight selected DE circRNAs in the left atrial appendage tissues of AF and SR patient groups. **B** Fold changes (AF vs. SR) in the expression levels of the eight circRNAs based on the transcriptome data. **C** Expression levels of the eight DE circRNAs in the peripheral blood of patients with SR and AF. **D–G** Receiver operating characteristic (ROC) curve analysis results show the diagnostic values of the 8 DE circRNAs for AF. AUC = area under the curve. *$p < 0.05$, **$p < 0.01$, and ***$p < 0.001$ compared with the SR group. AF, atrial fibrillation; SR, sinus rhythm

explore new mechanisms of AF pathogenesis and may reveal new diagnostic biomarkers or therapeutic targets.

This study has a few limitations. First, the sample size for sequencing was small, which reduced the integrity of the transcriptome data and the accuracy of target screening. Second, the functions of circRNAs in the development and prognosis of AF in vivo and in vitro have not been explored. Therefore, further investigations in animal and cell models are necessary to determine the roles of various ceRNA networks. Finally, this study investigated only circRNA functions via a ceRNA network and did not evaluate circRNAs on the basis of other functions, such as interactions with RNA-binding proteins. Therefore, further research should be conducted with respect to these limitations in the future.

Table 3 Selected DE circRNA-mRNAs in LAA tissues

CircRNA	FC	log2FC	p value	q value	Regulation	mRNAs	r	Regulation
circRNA_00324	8.593	3.103	2.14E-36	7.14E-35	Up	ANKRD33B/ABHD18/ENOX1/CR1/ATRNL1	0.855–0.963	Up
circRNA_17225	6.272	2.649	2.29E-57	1.97E-55	Up	ANKRD33B/JAK3	0.831–0.884	Up
circRNA_16305	7.033	2.814	2.45E-76	3.27E-74	Up	ANKRD33B/ABHD18/ENOX1/CR1/ATRNL1/ECT2L	0.830–0.967	Up
circRNA_10233	0.001	-9.550	1.93E-61	1.93E-59	Down	KCNA6/STC2	0.940–0.960	Down
circRNA_05499	3.644	1.866	1.02E-59	9.36E-58	Up	ANKRD33B/LBH	0.918–0.927	Up
circRNA_03183	2.266	1.180	1.28E-52	9.34E-51	Up	ENOX1/JAK3/ECT2L	0.805–0.926	Up
circRNA_14211	2.090	1.063	1.71E-29	3.14E-28	Up	ABHD18/ENOX1/CR1/ECT2L	0.847–0.981	Up
circRNA_18422	2.426	1.279	8.74E-08	1.85E-07	Up	ANKRD33B/TNFRSF11B/OSCAR/VDR	0.801–0.822	Up

DE, differentially expressed; LAA, left atrial appendage; FC, fold change; r, correlation coefficient

Table 4 The baseline demographic characteristics of the patients

Characteristics	SR patients (n = 21)	AF patients (n = 21)	*p*-value
Age (years)	58.81 ± 2.45	57.24 ± 2.12	0.630
Male, n (%)	12 (57.14)	12 (57.14)	1.000
BMI (kg/m^2)	25.94 ± 0.67	26.73 ± 0.96	0.504
Hypertension, n (%)	9 (42.86)	6 (28.57)	0.334
Diabetes mellitus, n (%)	3 (14.29)	1 (4.76)	0.599
Smoking, n (%)	8 (38.10)	5 (23.81)	0.317
Drinking, n (%)	6 (28.57)	3 (14.29)	0.452
HR (bpm)	73.57 ± 2.62	101.30 ± 5.14	< 0.0001
SBP (mmHg)	137.50 ± 4.19	128.50 ± 3.82	0.120
DBP (mmHg)	84.14 ± 2.55	84.00 ± 2.52	0.968
Leukocyte (10^9/L)	6.51 ± 0.39	6.09 ± 0.32	0.409
Hemoglobin (g/L)	136.80 ± 3.45	139.00 ± 3.63	0.664
Platelet (10^9/L)	231.3 ± 14.87	211.6 ± 12.70	0.319
TC (mmol/L)	4.52 ± 0.19	4.04 ± 0.22	0.108
TG (mmol/L)	1.39 ± 0.12	1.57 ± 0.28	0.572
HDL-C (mmol/L)	1.32 ± 0.06	1.20 ± 0.04	0.077
LDL-C (mmol/L)	2.82 ± 0.14	2.74 ± 0.15	0.690
LAD (mm)	34.71 ± 0.95	44.33 ± 1.41	< 0.0001
LVEF (%)	61.05 ± 0.57	57.95 ± 1.43	0.052
Medication			
ACEI/ARB/ARNI, n (%)	1 (4.76)	2 (9.52)	> 0.99
B-Blockers, n (%)	3 (14.29)	6 (28.57)	0.452
CCB, n (%)	3 (14.29)	3 (14.29)	1.000
Lipid-lowering drugs, n (%)	6 (28.57)	6 (28.57)	1.000
Antiarrhythmic drug, n (%)	0 (0)	2 (9.52)	0.488

SR, sinus rhythm; AF, atrial fibrillation; BMI, body mass index; HR, heart rate; SBP, systolic blood pressure; DBP, diastolic blood pressure; TC, total cholesterol; TG, total glyceride; HDL-C, high-density lipoprotein cholesterol; LDL-C, low-density lipoprotein cholesterol; LAD, left atrial diameter; LVEF, left ventricular ejection fractions; ACEI, angiotensin converting enzyme inhibitor; ARB, angiotensin II receptor blocker; ARNI, Angiotensin Receptor & Neprilysin Inhibitor, Sacubitril Valsartan; CCB, calcium channel blocker. The data are presented as means ± SEMs or number (%)

Conclusions

In this study, we systematically identified DE circRNAs in AF patients and characterised an AF-related ceRNA regulatory network. The mechanisms of action of the AF-related ceRNAs were elucidated through functional enrichment analysis. In this study, we also identified eight circRNAs as potential predictive biomarkers of AF. Our findings provide new research directions for understanding the pathogenetic mechanism of AF at the ceRNA level.

Table 5 ROC curve evaluation for the independent predictors of AF

CircRNA	AUC	95% CI	*p* values
circRNA_00324	0.9138	0.8323–0.9953	< 0.0001
circRNA_17225	0.7370	0.5857–0.8882	0.0086
circRNA_16305	0.8526	0.7377–0.9675	< 0.0001
circRNA_10233	0.6803	0.5147–0.8458	0.0455
circRNA_05499	0.8163	0.6903–0.9424	0.0004
circRNA_03183	0.8662	0.7614–0.9710	< 0.0001
circRNA_14211	0.7664	0.6249–0.9080	0.0031
circRNA_18422	0.9320	0.8597–1.000	< 0.0001

ROC, receiver operating characteristic; AF, atrial fibrillation; AUC, area under the curve; CI, confidence interval

Abbreviations

AF	Atrial fibrillation
circRNA	Circular RNA
LAA	Left atrial appendage
GO	Gene ontology
KEGG	Kyoto Encyclopaedia of Genes and Genomes
hsa	*Homo sapiens*
miRNA	MicroRNA
mRNA	Messenger RNA

Supplementary Information

The online version contains supplementary material available at https://doi.org/10.1186/s40246-025-00760-7.

Additional file 1.

Additional file 2.

Additional file 3.

Acknowledgements
None.

Author contributions
All authors contributed to the study conception and design. MW, BD, and JZ designed the experiments; MW, YC, and WY performed the experiments, analyzed the data, and were responsible for writing the manuscript; XL, GL, XW, and SL collected the clinical samples and the baseline data; GG, FM, and FK helped with the data analysis; DS and WQ revised the manuscript. All authors read and approved the final manuscript.

Funding
This work was funded by the Postdoctoral Program of Affiliated Hospital of Jining Medical University (NO. JYFY363230), the PhD Research Foundation of the Affiliated Hospital of Jining Medical University (NO. 2021-BS-005), the Nursery Research Project of the Affiliated Hospital of Jining Medical University (NO. MP-ZD-2022-001), the Shandong Postdoctoral Science Foundation (NO. SDCX-ZG-202400021), the Project of Medicine Health and Technology Program of Shandong Province (NO. 202303010408), the Shandong Province Universities's Plan for Youth Innovation Teams (NO. 2022KJ103), and the Program of Taishan Scholars Programme (NO. ts 20190979).

Data availability
Data is provided within the manuscript or supplementary information files.

Declarations

Ethics approval and consent to participate
This study was performed in accordance with the Declaration of Helsinki, and the research protocol was approved by the Ethics Committee of the Affiliated Hospital of Jining Medical University (approval number 2021B116). Written informed consent was obtained from all participants.

Competing interests
The authors declare no competing interests.

Author details
[1]Shandong Provincial Key Medical and Health Discipline of Cardiology, Jining Key Laboratory for Diagnosis and Treatment of Cardiovascular Diseases, Jining Key Laboratory of Precise Therapeutic Research of Coronary Intervention, Department of Cardiology, Affiliated Hospital of Jining Medical University, Jining, Shandong, China. [2]Postdoctoral Mobile Station of Shandong University of Traditional Chinese Medicine, Jinan, Shandong, China. [3]Department of Medical Record, Affiliated Hospital of Jining Medical University, Jining, Shandong, China. [4]Department of Laboratory Medicine, Affiliated Hospital of Jining Medical University, Jining, Shandong, China. [5]School of Pharmacy, Jining Medical University, Rizhao, Shandong, China. [6]Department of Cardiology, Shandong Provincial Hospital Affiliated to Shandong First Medical University, Jinan, Shandong, China.

Received: 15 October 2024 Accepted: 21 April 2025
Published online: 12 May 2025

References

1. Hindricks G, Potpara T, Dagres N, Arbelo E, Bax JJ, Blomström-Lundqvist C, et al. 2020 ESC Guidelines for the diagnosis and management of atrial fibrillation developed in collaboration with the European Association for Cardio-Thoracic Surgery (EACTS): The Task Force for the diagnosis and management of atrial fibrillation of the European Society of Cardiology (ESC) Developed with the special contribution of the European Heart Rhythm Association (EHRA) of the ESC. Eur Heart J. 2021;42(5):373–498. https://doi.org/10.1093/eurheartj/ehaa612.
2. Roth GA, Mensah GA, Johnson CO, Addolorato G, Ammirati E, Baddour LM, et al. Global Burden of Cardiovascular Diseases and Risk Factors, 1990–2019: Update From the GBD 2019 Study. J Am Coll Cardiol. 2020;76(25):2982–3021. https://doi.org/10.1016/j.jacc.2020.11.010.
3. Suzuki H, Tsukahara T. A view of pre-mRNA splicing from RNase R resistant RNAs. Int J Mol Sci. 2014;15(6):9331–42. https://doi.org/10.3390/ijms15069331.
4. Wang C, Liu H. Factors influencing degradation kinetics of mRNAs and half-lives of microRNAs, circRNAs, lncRNAs in blood in vitro using quantitative PCR. Sci Rep. 2022;12(1):7259. https://doi.org/10.1038/s41598-022-11339-w.
5. Tay Y, Rinn J, Pandolfi P. The multilayered complexity of ceRNA crosstalk and competition. Nature. 2014;505(7483):344–52. https://doi.org/10.1038/nature12986.
6. Zhang Z, Yang T, Xiao J. Circular RNAs: promising biomarkers for human diseases. EBioMedicine. 2018;34:267–74. https://doi.org/10.1016/j.ebiom.2018.07.036.
7. Lin J, Wang X, Zhai S, Shi M, Peng C, Deng X, et al. Hypoxia-induced exosomal circPDK1 promotes pancreatic cancer glycolysis via c-myc activation by modulating miR-628-3p/BPTF axis and degrading BIN1. J Hematol Oncol. 2022;15(1):128. https://doi.org/10.1186/s13045-022-01348-7.
8. Xueqi L, Jiang L, Zeng H, Gao L, Guo S, Chen C, et al. Circ-0000953 deficiency exacerbates podocyte injury and autophagy disorder by targeting Mir665-3p-Atg4b in diabetic nephropathy. Autophagy. 2024;20(5):1072–97. https://doi.org/10.1080/15548627.2023.2286128.
9. Chen B, Yi J, Xu Y, Zheng P, Tang R, Liu B. Construction of a circRNA-miRNA-mRNA network revealed the potential mechanism of Buyang Huanwu Decoction in the treatment of cerebral ischemia. Biomed Pharmacother. 2022;145: 112445. https://doi.org/10.1016/j.biopha.2021.112445.

10. Gao Y, Wang J, Zhao F. CIRI: an efficient and unbiased algorithm for de novo circular RNA identification. Genome Biol. 2015;16(1):4. https://doi.org/10.1186/s13059-014-0571-3.
11. Quinlan AR. BEDTools: the swiss-army tool for genome feature analysis. Curr Protoc Bioinform. 2014. https://doi.org/10.1002/0471250953.bi1112s47.
12. Wang L, Feng Z, Wang X, Wang X, Zhang X. DEGseq: an R package for identifying differentially expressed genes from RNA-seq data. Bioinformatics. 2010;26(1):136–8. https://doi.org/10.1093/bioinformatics/btp612.
13. John B, Enright AJ, Aravin A, Tuschl T, Sander C, Marks DS. Human MicroRNA targets. PLoS Biol. 2004;2(11): e363. https://doi.org/10.1371/journal.pbio.0020363.
14. Tay Y, Kats L, Salmena L, Weiss D, Tan SM, Ala U, et al. Coding-independent regulation of the tumor suppressor PTEN by competing endogenous mRNAs. Cell. 2011;147(2):344–57. https://doi.org/10.1016/j.cell.2011.09.029.
15. Salmena L, Poliseno L, Tay Y, Kats L, Pandolfi PP. A ceRNA hypothesis: the Rosetta Stone of a hidden RNA language? Cell. 2011;146(3):353–8. https://doi.org/10.1016/j.cell.2011.07.014.
16. Vanhaverbeke M, Vausort M, Veltman D, Zhang L, Wu M, Laenen G, et al. Peripheral blood RNA levels of QSOX1 and PLBD1 are new independent predictors of left ventricular dysfunction after acute myocardial infarction. Circ Genom Precis Med. 2019;12(12): e002656. https://doi.org/10.1161/CIRCGEN.119.002656.
17. Ford E, Ares M Jr. Synthesis of circular RNA in bacteria and yeast using RNA cyclase ribozymes derived from a group I intron of phage T4. Proc Natl Acad Sci U S A. 1994;91(8):3117–21. https://doi.org/10.1073/pnas.91.8.3117.
18. Li P, Zhu K, Mo Y, Deng X, Jiang X, Shi L, et al. Research progress of circRNAs in head and neck cancers. Front Oncol. 2021;11: 616202. https://doi.org/10.3389/fonc.2021616202.
19. Cen L, Liu R, Liu W, Li Q, Cui H. Competing endogenous RNA networks in glioma. Front Genet. 2021;12: 675498. https://doi.org/10.3389/fgene.2021.675498.
20. Okholm TLH, Sathe S, Park SS, Kamstrup AB, Rasmussen AM, Shankar A, et al. Transcriptome-wide profiles of circular RNA and RNA-binding protein interactions reveal effects on circular RNA biogenesis and cancer pathway expression. Genome Med. 2020;12(1):112. https://doi.org/10.1186/s13073-020-00812-8.
21. Zhang Y, Zhang XO, Chen T, Xiang JF, Yin QF, Xing YH, et al. Circular intronic long noncoding RNAs. Mol Cell. 2013;51(6):792–806. https://doi.org/10.1016/j.molcel.2013.08.017.
22. Sinha T, Panigrahi C, Das D, Chandra PA. Circular RNA translation, a path to hidden proteome. Wiley Interdiscip Rev RNA. 2022;13(1): e1685. https://doi.org/10.1002/wrna.1685.
23. Madè A, Bibi A, Garcia-Manteiga JM, Tascini AS, Piella SN, Tikhomirov R, et al. circRNA-miRNA-mRNA deregulated network in ischemic heart failure patients. Cells. 2023;12(21):2578. https://doi.org/10.3390/cells12212578.
24. Yang M, Wang W, Wang L, Li Y. Circ_0001052 promotes cardiac hypertrophy via elevating Hipk3. Aging (Albany NY). 2023;15(4):1025–38. https://doi.org/10.18632/aging.204521.
25. Brundel BJJM, Ai X, Hills MT, Kuipers MF, Lip GYH, de Groot NMS. Atrial fibrillation. Nat Rev Dis Primers. 2022;8(1):21. https://doi.org/10.1038/s41572-022-00347-9.
26. Burg S, Attali B. Targeting of potassium channels in cardiac arrhythmias. Trends Pharmacol Sci. 2021;42(6):491–506. https://doi.org/10.1016/j.tips.2021.03.005.
27. Thibault S, Long V, Fiset C. Higher Na^+-Ca^{2+} exchanger function and triggered activity contribute to male predisposition to atrial fibrillation. Int J Mol Sci. 2022;23(18):10724. https://doi.org/10.3390/ijms231810724.
28. Wu N, Li C, Xu B, Xiang Y, Jia X, Yuan Z, et al. Circular RNA mmu_circ_0005019 inhibits fibrosis of cardiac fibroblasts and reverses electrical remodeling of cardiomyocytes. BMC Cardiovasc Disord. 2021;21(1):308. https://doi.org/10.1186/s12872-021-02128-w.
29. Li GR, Sun HY, Chen JB, Zhou Y, Tse HF, Lau CP. Characterization of multiple ion channels in cultured human cardiac fibroblasts. PLoS ONE. 2009;4(10): e7307. https://doi.org/10.1371/journal.pone.0007307.
30. Han Y, Chen JD, Liu ZM, Zhou Y, Xia JH, Du XL, et al. Functional ion channels in mouse cardiac c-kit(+) cells. Am J Physiol Cell Physiol. 2010;298(5):C1109–17. https://doi.org/10.1152/ajpcell.00207.2009.
31. Zeiger W, Ito D, Swetlik C, Oh-hora M, Villereal ML, Thinakaran G. Stanniocalcin 2 is a negative modulator of store-operated calcium entry. Mol Cell Biol. 2011;31(18):3710–22. https://doi.org/10.1128/MCB.05140-11.
32. Fleet JC. Vitamin D-mediated regulation of intestinal calcium absorption. Nutrients. 2022;14(16):3351. https://doi.org/10.3390/nu14163351.
33. Song Y, Kato S, Fleet JC. Vitamin D receptor (VDR) knockout mice reveal VDR-independent regulation of intestinal calcium absorption and ECaC2 and calbindin D9k mRNA. J Nutr. 2003;133(2):374–80. https://doi.org/10.1093/jn/133.2.374.
34. Meng A, Wei S, Yan L, Xiao Y, Ding Z, Feng Y. Bioinformatic analysis and validation of cardiac hypertrophy-related genes. Gen Physiol Biophys. 2023;42(2):159–67. https://doi.org/10.4149/gpb_2022059.
35. Steinbeck MJ, Appel WH Jr, Verhoeven AJ, Karnovsky MJ. NADPH-oxidase expression and in situ production of superoxide by osteoclasts actively resorbing bone. J Cell Biol. 1994;126(3):765–72. https://doi.org/10.1083/jcb.126.3.765.
36. Ramos-Mondragón R, Lozhkin A, Vendrov AE, Runge MS, Isom LL, Madamanchi NR. NADPH oxidases and oxidative stress in the pathogenesis of atrial fibrillation. Antioxidants (Basel). 2023;12(10):1833. https://doi.org/10.3390/antiox12101833.
37. O'Neal WT, Lakoski SG, Qureshi W, Judd SE, Howard G, Howard VJ, et al. Relation between cancer and atrial fibrillation (from the REasons for Geographic And Racial Differences in Stroke Study). Am J Cardiol. 2015;115(8):1090–4. https://doi.org/10.1016/j.amjcard.2015.01.540.
38. Gawlik M, Zimodro JM, Gąsecka A, Filipiak KJ, Szmit S. Cardiac arrhythmias in oncological patients-epidemiology, risk factors, and management within the context of the new ESC 2022 guidelines. Curr Oncol Rep. 2023;25(10):1107–15. https://doi.org/10.1007/s11912-023-01445-x.
39. Madnick DL, Fradley MG. Atrial fibrillation and cancer patients: mechanisms and management. Curr Cardiol Rep. 2022;24(10):1517–27. https://doi.org/10.1007/s11886-022-01769-3.
40. Li S, Jiang Z, Chao X, Jiang C, Zhong G. Identification of key immune-related genes and immune infiltration in atrial fibrillation with valvular heart disease based on bioinformatics analysis. J Thorac Dis. 2021;13(3):1785–98. https://doi.org/10.21037/jtd-21-168.
41. Yao Y, Yang M, Liu D, Zhao Q. Immune remodeling and atrial fibrillation. Front Physiol. 2022;13: 927221. https://doi.org/10.3389/fphys.2022.927221.
42. Hessvik NP, Llorente A. Current knowledge on exosome biogenesis and release. Cell Mol Life Sci. 2018;75(2):193–208. https://doi.org/10.1007/s00018-017-2595-9.
43. Tang Y, Bao J, Hu J, Liu L, Xu DY. Circular RNA in cardiovascular disease: expression, mechanisms and clinical prospects. J Cell Mol Med. 2021;25(4):1817–24. https://doi.org/10.1111/jcmm.16203.
44. Wang R, Bektik E, Sakon P, Wang X, Huang S, Meng X, et al. Integrated analysis of the microRNA-mRNA network predicts potential regulators of atrial fibrillation in humans. Cells. 2022;11(17):2629. https://doi.org/10.3390/cells11172629.
45. Hu J, Wang X, Cui X, Kuang W, Li D, Wang J. Quercetin prevents isoprenaline-induced myocardial fibrosis by promoting autophagy via regulating miR-223-3p/FOXO3. Cell Cycle. 2021;20(13):1253–69. https://doi.org/10.1080/15384101.2021.1932029.
46. Venkateswaran A, Sekhar KR, Levic DS, Melville DB, Clark TA, Rybski WM, et al. The NADH oxidase ENOX1, a critical mediator of endothelial cell radiosensitization, is crucial for vascular development. Cancer Res. 2014;74(1):38–43. https://doi.org/10.1158/0008-5472.CAN-13-1981.
47. Karam BS, Chavez-Moreno A, Koh W, Akar JG, Akar FG. Oxidative stress and inflammation as central mediators of atrial fibrillation in obesity and diabetes. Cardiovasc Diabetol. 2017;16(1):120. https://doi.org/10.1186/s12933-017-0604-9.

Publisher's Note

Springer Nature remains neutral with regard to jurisdictional claims in published maps and institutional affiliations.